

Flip-angle-optimized fast dynamic T₁ mapping with a 3D gradient-echo sequence

Olaf Dietrich^{1†}, Maximilian Freiermuth^{1†}, Linus Willerding², Maximilian F. Reiser¹, Michael Peller¹

¹ Josef Lissner Laboratory for Biomedical Imaging, Institute for Clinical Radiology, Ludwig-Maximilians-University Hospital Munich, Germany

² Department of Internal Medicine III, Ludwig-Maximilians-University Hospital Munich, Germany

† Olaf Dietrich and Maximilian Freiermuth contributed equally to this work.

ELECTRONIC PREPRINT VERSION:

This is the peer reviewed version of the following article: *Magn Reson Med* 2015; **73**(3): 1158–1163, which has been published in final form at <URL:<http://dx.doi.org/10.1002/mrm.25199>>.

This article may be used for non-commercial purposes in accordance with [Wiley Terms and Conditions for Self-Archiving](#).

Abstract

Purpose: To analyze the flip-angle dependence and to optimize the statistical precision of a fast three-dimensional T₁-mapping technique based on the variable-flip-angle (VFA) method. The proposed single-flip-angle (1FA) approach acquires only a single 3D spoiled gradient-echo data set for each time point of the dynamical series in combination with a longer baseline measurement.

Theory and Methods: The optimal flip angle for the dynamic series can be calculated as $\alpha_{\text{dyn,opt}} = \arccos[(2E_1 - 1)/(2 - E_1)]$ (with $E_1 = \exp(-T_R/T_1)$) by minimizing the statistical error of T₁. T₁ maps of a liquid phantom with stepwise increasing concentrations of contrast-agent were measured using a saturation-recovery (SR) and a VFA/1FA technique with 11 flip angles. The standard deviation of the parameter maps was defined as statistical error of the 1FA measurement.

Results: The measured statistical error of the 1FA technique as a function of α_{dyn} agrees well with the derived theoretical curve. The optimal flip angle increases from about 5° for T₁=2629 ms to 30° for T₁=137 ms. The relative deviation be-

tween 1FA and SR measurements varies between -2.9 % and +10.3 %. Measurements in vivo confirm the expression for the optimal flip angle.

Conclusion: The proposed flip-angle-optimized 1FA technique optimizes the precision of T₁ values in dynamic phantom measurements.

Key words:

Magnetic resonance imaging; Longitudinal relaxation time T₁; Fast, dynamic imaging; Contrast agent concentration

Corresponding author:

Olaf Dietrich, PhD
Josef Lissner Laboratory for Biomedical Imaging
Institute for Clinical Radiology
Ludwig-Maximilians-University Hospital Munich
Marchioninstr. 15
81377 Munich
Germany
Phone: +49 89 7095-4622
Fax: +49 89 7095-4627
E-mail: od@dtrx.net

Introduction

Fast mapping of the longitudinal MR relaxation time constant (T_1) is of considerable interest for many different MRI applications and several different approaches for T_1 mapping have been proposed in the past (1-6). Fast dynamic T_1 mapping methods with temporal resolutions in the order of seconds are desirable in particular for the rapid quantification of contrast-agent concentrations. Dynamically acquired contrast-agent concentrations are of interest, e. g., for an improved quantification of hemodynamic parameters such as blood flow or blood volume in dynamic contrast-enhanced perfusion MRI (DCE-MRI) (7).

The most frequently used approaches for T_1 mapping are saturation-recovery (SR) or inversion-recovery (IR) experiments with different recovery times (1), Look-Locker-like experiments (2, 3), IR snapshot fast low-angle-shot (snapshot FLASH) experiments (4), or fast gradient-echo techniques with variable flip angles (VFA) (5, 6).

The purpose of the present study was to analyze the flip-angle dependence and to optimize the statistical precision of a fast three-dimensional T_1 mapping approach based on the VFA technique, in which only a single 3D gradient-echo data set for each time point of the dynamical series is acquired.

Theory

The conventional VFA technique is based on the acquisition of at least two (but frequently more) gradient-echo data sets with different flip angles – typically in a range between 2° and 30° (5). The signal, S , of each acquisition is given by the FLASH equation (4)

$$S = S_0 \sin(\alpha) \frac{1-E_1}{1-E_1 \cos(\alpha)} E_2, \quad [1]$$

where S_0 is the signal (magnetization) after full longitudinal relaxation, α the flip angle, $E_1 = \exp(-T_R/T_1)$, and $E_2 = \exp(-T_E/T_2^*)$. E_1 (and, hence, the relaxation time constant $T_1 = -T_R / \ln E_1$) can be obtained from at least 2 signals $S(\alpha)$ acquired at different flip angles by solving the corresponding system of linear equations for the 2 unknown variables E_1 and $S_0 E_2$.

For dynamic applications with high temporal resolutions, this approach can be accelerated by combining a longer baseline acquisition with multiple flip angles (prior to the actual dynamic acquisi-

tion) and a fast repeated acquisition with only a single flip angle for the dynamic phase (8). The baseline acquisition is used to determine the value of S_0 . The signal intensity, S_{dyn} , of the subsequent single-flip-angle (1FA) acquisitions with flip angle α_{dyn} can be used to determine $E_{1,\text{dyn}}$ (and $T_{1,\text{dyn}}$) by inversion of Eq. [1] if S_0 is known:

$$E_{1,\text{dyn}} = \frac{S_0 E_2 \sin(\alpha_{\text{dyn}}) - S_{\text{dyn}}}{S_0 E_2 \sin(\alpha_{\text{dyn}}) - S_{\text{dyn}} \cos(\alpha_{\text{dyn}})} \approx \frac{S_0 \sin(\alpha_{\text{dyn}}) - S_{\text{dyn}}}{S_0 \sin(\alpha_{\text{dyn}}) - S_{\text{dyn}} \cos(\alpha_{\text{dyn}})}. \quad [2]$$

The shown approximation is based on neglecting the T_2^* dependence for sufficiently short echo times T_E , i. e., for $E_2 \approx 1$.

The optimal flip angle, α_{dyn} , for the dynamic phase can be determined by minimizing the statistical error, $\Delta E_{1,\text{dyn}}$, of $E_{1,\text{dyn}}$. In general, this error is given by

$$\Delta E_{1,\text{dyn}} = \sqrt{\left(\left| \frac{\partial E_{1,\text{dyn}}}{\partial S_{\text{dyn}}} \right| \Delta S_{\text{dyn}} \right)^2 + \left(\left| \frac{\partial E_{1,\text{dyn}}}{\partial S_0} \right| \Delta S_0 \right)^2}. \quad [3]$$

Assuming sufficient time for a precise baseline measurement of the fully relaxed signal S_0 and, thus, considering only the influence of errors, ΔS_{dyn} , of the measured dynamic signal intensity, S_{dyn} , the statistical error of $E_{1,\text{dyn}}$ is in good approximation

$$\Delta E_{1,\text{dyn}} \approx \left| \frac{\partial E_{1,\text{dyn}}}{\partial S_{\text{dyn}}} \right| \Delta S_{\text{dyn}} = \frac{S_0 \sin(\alpha_{\text{dyn}}) (1 - \cos(\alpha_{\text{dyn}}))}{(S_0 \sin(\alpha_{\text{dyn}}) - S_{\text{dyn}} \cos(\alpha_{\text{dyn}}))^2} \Delta S_{\text{dyn}} \quad [4]$$

and, after replacing S_{dyn} by the expression in Eq. [1]

$$\Delta E_{1,\text{dyn}} \approx \frac{(1 - E_{1,\text{dyn}} \cos(\alpha_{\text{dyn}}))^2}{S_0 \sin(\alpha_{\text{dyn}}) (1 - \cos(\alpha_{\text{dyn}}))} \Delta S_{\text{dyn}}. \quad [5]$$

This statistical error is shown in Fig. 1 and has – as a function of α_{dyn} for given $E_{1,\text{dyn}}$ – a unique minimum defining the optimal flip angle, $\alpha_{\text{dyn,opt}}$, for dynamic T_1 measurements, which can be calculated as the zero of the derivative $\frac{\partial}{\partial \alpha_{\text{dyn}}} \Delta E_{1,\text{dyn}}(\alpha_{\text{dyn}}) = 0$:

$$\alpha_{\text{dyn,opt}} = \arccos \frac{2E_1 - 1}{2 - E_1}. \quad [6]$$

It is interesting to note that $\alpha_{\text{dyn,opt}}$ lies always above the Ernst angle $\alpha_{\text{Ernst}} = \arccos(E_1)$ (9) by about 33 % to 73 %; cf. Fig. 1.

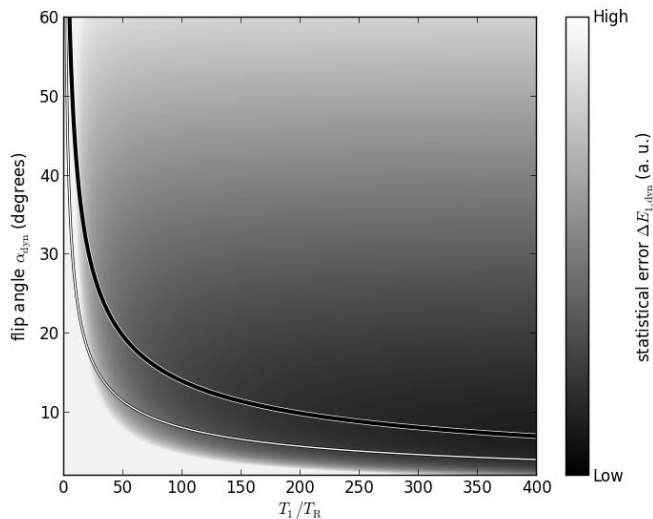


Figure 1: Statistical error $\Delta E_{1,dyn}$ (grey-scaled) of dynamic $E_{1,dyn}$ (and T_1) measurement with the single-flip-angle approach as a function of T_1/T_R and of the flip angle α_{dyn} . The minimum error (i. e., the optimal flip angle) as a function of T_1/T_R is indicated by the thick black line. For comparison, the Ernst angle is shown as thinner white line.

Methods

The proposed single-acquisition method for dynamic T_1 quantification was evaluated in phantom measurements on a 3-Tesla whole-body MRI scanner (Magnetom Verio, Siemens Healthcare, Erlangen, Germany) using a liquid phantom with step-wise increased concentrations of gadolinium contrast agent (gadobutrol, Gadovist, Bayer Schering Pharma, Berlin, Germany). The phantom was based on physiological saline solution and the contrast-agent concentration was varied in 7 steps from 0 to about 1.2 mmol/L.

3D spoiled gradient-echo measurements were performed at each step with 11 flip angles: $\alpha_{dyn} = 2.5^\circ, 5.0^\circ, 7.5^\circ, 10.0^\circ, 12.5^\circ, 15.0^\circ, 17.5^\circ, 20.0^\circ, 22.5^\circ, 25.0^\circ, \text{ and } 30.0^\circ$. Other sequence parameters were: $T_R = 7.0$ ms, $T_E = 3.0$ ms, matrix = $128 \times 128 \times 48$, spatial resolution: $1.44 \times 1.44 \times 4$ mm³, receiver bandwidth = 391 Hz/pixel, RF phase spoiling increment: 33° . The scan time for each of the 11 3D data sets was 43 s. The B_1 field was measured for flip-angle correction with the ‘actual flip-angle imaging’ (AFI) method (10); sequence parameters were $T_{R,1} = 20$ ms, $T_{R,2} = 100$ ms, $T_E = 5.0$ ms, flip angle $\alpha = 60^\circ$, matrix = $64 \times 64 \times 48$, spatial resolution: $2.88 \times 2.88 \times 4$ mm³, receiver bandwidth = 391 Hz/pixel, RF phase spoiling increment:

33° , spoiler gradient duration of 12 ms (in $T_{R,1}$) and 61 ms (in $T_{R,2}$); resulting in a scan time of 6:08 min. As reference, T_1 was determined using a 2D saturation-recovery (SR) measurement based on a turbo-FLASH sequence; the protocol parameters were $T_R = 2.7$ ms, $T_E = 1.3$ ms, 17 recovery times $T_{rec} = 71, 171, 271, 371, 471, 571, 671, 771, 871, 971, 1210, 1460, 1710, 1960, 2460, 2960, 4960$ ms, flip angle $\alpha = 15^\circ$, matrix = $128 \times 128 \times 24$, spatial resolution: $1.44 \times 1.44 \times 6$ mm³, receiver bandwidth = 737 Hz/pixel. The total scan time for all 17 saturation-recovery experiments was about 12 minutes in each of the 7 experimental steps.

T_1 maps were calculated for each of the 7 experimental steps with increasing Gd concentrations using the saturation-recovery data sets (7×1 T_1 map based on 17 recovery times), the complete VFA data sets (7×1 T_1 map based on all 11 flip angles), and finally for each single flip angle (7×1 T_1 maps) using the proposed 1FA technique and the S_0 map of the VFA evaluation of step 0. For the VFA and 1FA evaluation, the flip angle was corrected on a pixel-by-pixel basis based on the AFI B_1 measurements. T_1 was determined by pixelwise non-linear fitting of the SR and FLASH equation to the acquired data for the SR and VFA measurements, respectively; for the 1FA measurements, T_1 was determined directly using Eq. [2].

The quantitative evaluation was based on a box-shaped region of interest of $20 \times 34 \times 18 = 12,240$ pixels in the VFA/1FA maps and $20 \times 34 \times 12 = 8,160$ pixels in the SR maps; the latter region extends over fewer slices because of the larger slice thickness. The statistical error of the 1FA method was assessed (and compared to the theory) using the spatial standard deviation of the T_1 maps in this region; to evaluate the precision of this estimate, the aforementioned region was subdivided into 8 octants, standard deviations within each octant were calculated separately, and then mean values and standard deviations of these 8 values were determined. The systematic error of T_1 mapping was assessed using the T_1 mean value (and its standard deviation) over the complete region and its relative deviation from the SR reference measurements.

To demonstrate the applicability of the flip-angle optimization in vivo, an additional series of 3D spoiled gradient-echo measurements of the head of a healthy volunteer (who gave written in-

formed consent to this study) was acquired on a 1.5-Tesla whole-body MRI scanner (Magnetom Avanto, Siemens Healthcare, Erlangen, Germany) with 13 flip angles: $\alpha_{\text{dyn}} = 1.0^\circ, 2.5^\circ, 5.0^\circ, 7.5^\circ, \dots, 30.0^\circ$. Other sequence parameters were: $T_R = 5.0$ ms, $T_E = 1.2$ ms, matrix = 128×128×80, spatial resolution: 2×2×2 mm³, receiver bandwidth = 488 Hz/pixel. T_1 maps were calculated using the VFA approach based on all 13 flip angles. Then, the brain was segmented from the dataset using the brain extraction tool (BET) of the FMRIB Software Library (FSL, Analysis Group, Oxford, UK) (11). Within the T_1 maps restricted to brain tissue, we defined 3 sets of pixels by T_1 thresholding: sample #1: 750 ms < T_1 < 850 ms, sample #2: 1050 ms < T_1 < 1150 ms, sample #3: 1350 ms < T_1 < 1450 ms. Using the S_0 map of the VFA evaluation, 1FA T_1 maps for each flip angle were calculated. Finally, for each of the 3 pixel samples defined above, the standard deviation of the difference of $T_{1,1\text{FA}}(\alpha_{\text{dyn}})$ and $T_{1,\text{VFA}}$ was determined and used as a surrogate quantity for the statistical error of the 1FA T_1 maps.

Results

The T_1 relaxation times of the liquid phantom decreased from about 2600 ms (step 0, no Gd added) to about 140 ms (step 6, highest concentration of Gd). The statistical error of the T_1 quantification (standard deviation of T_1 map) as a function of α_{dyn} for different relaxation times, T_1 , is plotted in Fig. 2a–g together with the (appropriately scaled) theoretical curve $\Delta E_{1,\text{dyn}}(\alpha_{\text{dyn}})$ (as given in Eq. [5]). The minima of both the measured errors and the theoretical curve agreed well and increased from about 5° for $T_1=2629$ ms to 30° for $T_1=137$ ms (Table 1). In Fig. 2h, the theoretical and experimentally determined optimal flip angles are compared in a Bland-Altman plot (12), which indicates a reasonable agreement with a small negative bias (about –2.5°) of the experimentally determined flip angles. The Spearman’s rank correlation ρ of these flip angles is 0.991 (p-value 0.000015).

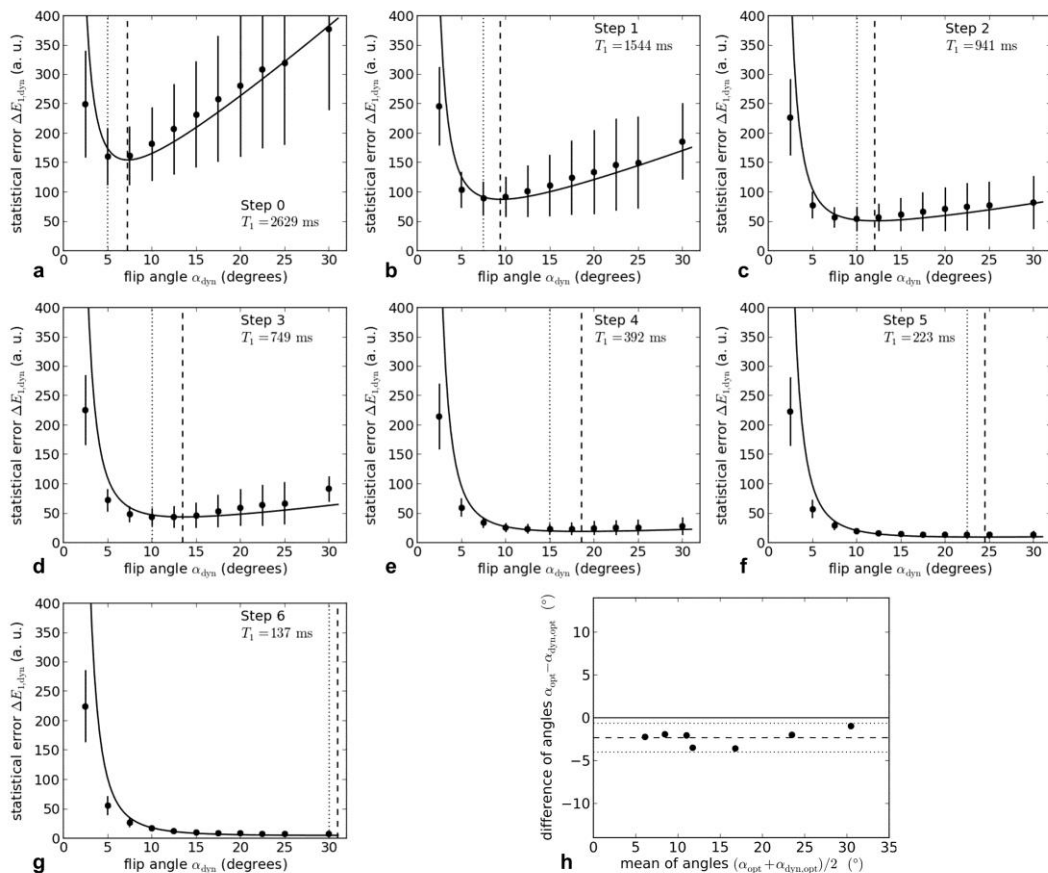


Figure 2: Measured statistical error (parameter standard deviation in T_1 maps, black circles with error bars) and scaled theoretical statistical error ($\Delta E_{1,\text{dyn}}$, solid black line) for 7 different relaxation times (a–g). The minima of the experimental and theoretical statistical errors are indicated by dotted and dashed vertical lines, respectively. (h) Bland-Altman plot of the theoretically ($\alpha_{\text{dyn,opt}}$) and experimentally (α_{opt}) optimal flip angle.

Table 1: Measured T_1 time constants (standard deviations) and optimal flip angles for 1FA measurements

	Step 0	Step 1	Step 2	Step 3	Step 4	Step 5	Step 6
T_1 (ms): SR (reference)	2629 (128)	1544 (38)	941 (16)	749 (12)	392 (6)	223 (4)	137 (3)
α_{opt} (experiment)	5.0°	7.5°	10.0°	10.0°	15.0°	22.5°	30.0°
$\alpha_{dyn,opt}$ (theory)	7.23°	9.43°	12.06°	13.50°	18.59°	24.50°	30.97°
T_1 (ms): 1FA ($\alpha_{dyn}=12.5^\circ$)	2901 (278)	1607 (142)	935 (79)	730 (60)	381 (32)	222 (20)	140 (15)
Relative deviation of T_1 (%)	+10.3	+4.0	-0.6	-2.6	-2.9	-0.2	+2.6

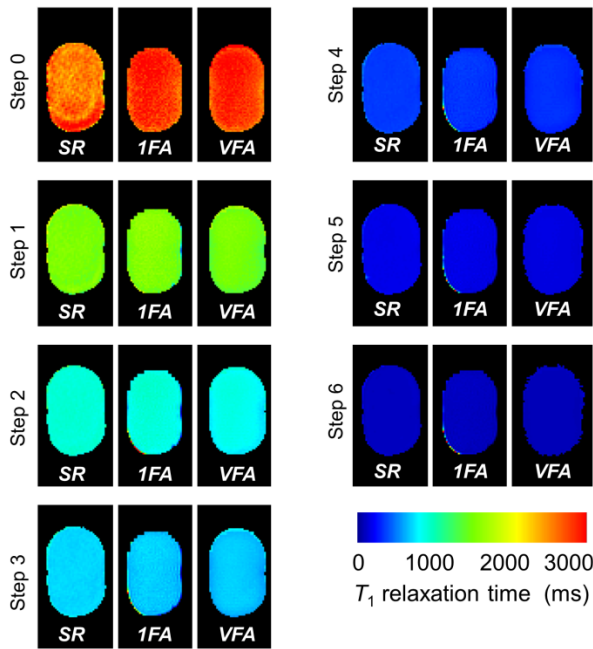


Figure 3: T_1 map comparison of saturation-recovery approach (SR, reference), the proposed single-flip-angle (1FA) approach with a flip angle of 12.5°, and the variable-flip-angle (VFA) approach with 11 flip angles between 2.5° and 30°. Background pixels with signal intensity below a threshold value are set to 0.

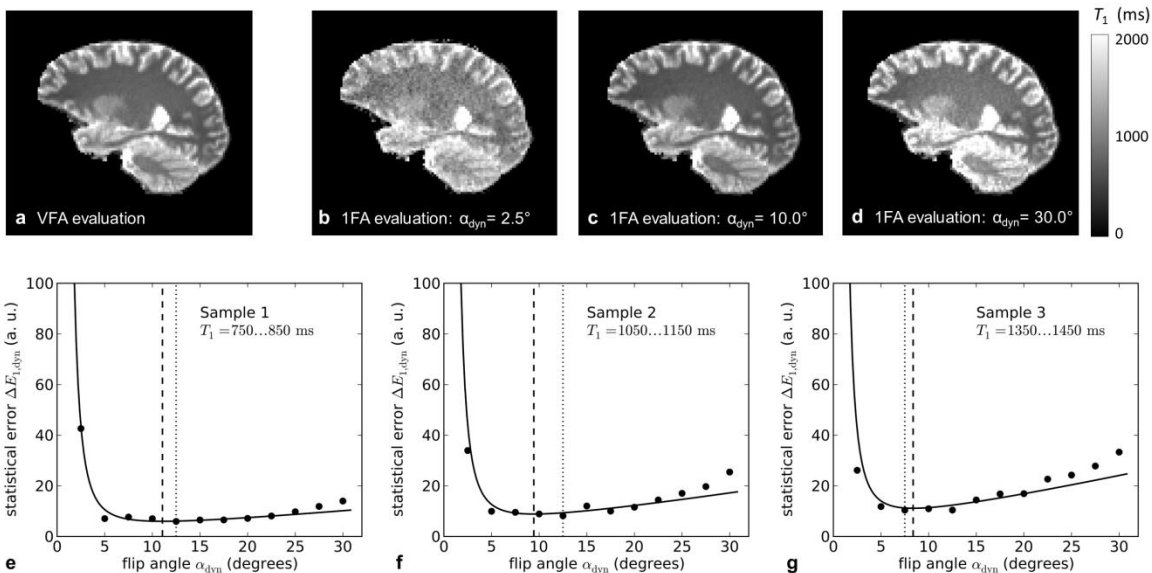


Figure 4: Statistical error of measurements *in vivo*. (a) VFA reference T_1 map based on 13 flip angles between 1° and 30°; (b–d) 1FA T_1 maps for 3 different flip angles of 2.5°, 10.0°, and 30.0°; (e–g) parameter standard deviation in T_1 maps (black circles) and scaled theoretical statistical error ($\Delta E_{1,dyn}$, solid black line) for 3 different sets of pixels (different relaxation time ranges). The minima of the experimental and theoretical statistical errors are indicated by dotted and dashed vertical lines, respectively.

The determined T_1 values of the SR and 1FA measurement with $\alpha_{\text{dyn}}=12.5^\circ$ (which is approximately the mean value of $\alpha_{\text{dyn,opt}}$ over the T_1 range from 140 to 2630 ms) are also listed in Table 1. The relative deviation between the 1FA measurements and the standard of reference varied between -2.9% and $+10.3\%$.

Parameter maps of T_1 determined with the saturation-recovery technique, the optimized 1FA approach, and with the conventional VFA technique (using all 11 flip angles) are shown in Fig. 3. The maps illustrate a good visual agreement of both methods.

In-vivo results are displayed in Fig. 4. T_1 maps illustrate that the statistical error of the 1FA maps increased for too small (2.5° , Fig. 4b) or too large (30.0° , Fig. 4d) flip angles, while the data quality obtained with a flip angle of 10.0° (Fig. 4c, the optimum for $T_R=5$ ms and T_1 relaxation times around 1000 ms as found in brain tissue) was similar to the quality of the VFA map (Fig. 4a). The estimated statistical errors as a function of the flip angle α_{dyn} as well as the optimal flip angles agreed well with the scaled theoretical curve (Fig. 4e–g) for all 3 analyzed ranges of T_1 ; the number of pixels of each evaluated T_1 range was $N=24,541$ for sample #1, $N=17,429$ for sample #2, and $N=16,597$ for sample #3.

Discussion

The rapid measurement of T_1 after contrast-agent administration based on a FLASH sequence with only a single flip angle has first been proposed by Brookes et al. in 1996 (8). Their theoretical analysis, however, is complicated by the fact that the statistical error is considered as a function of three flip angles (two flip angles applied prior to the dynamic phase and a third one used during the dynamic phase). In the present approach, we simplify the analysis by assuming the acquisition of a sufficiently large number of baseline measurements (before the dynamic phase) such that the statistical error of all baseline parameters can be neglected. Thus, the statistical error of the dynamic T_1 measurement depends only on the flip angle used during the dynamic phase and is given by a relatively simple expression somewhat similar to the Ernst angle equation: $\alpha_{\text{dyn,opt}} = \arccos[(2E_1 - 1)/(2 - E_1)]$. As shown in Fig. 1, the optimal flip angle for the 1FA

method is always greater than the Ernst angle; i. e., it is not the flip angle with the maximum available signal. Instead, it is basically the absolute change of the signal when varying T_1 that is maximized by this flip angle.

This theoretically derived optimal flip angle could be experimentally confirmed by the presented results in a liquid phantom with varying T_1 relaxation times and in vivo: the flip angle with minimal statistical error (parameter noise) in the experiments agrees well with the theoretical optimal flip angle $\alpha_{\text{dyn,opt}}$ (Table 1, Figs. 2 and 4). The remaining small but systematic deviations of the measured optimal flip angle in the phantom displayed in the Bland-Altman plot (Fig. 2h) have two explanations. (a) The discrete flip angle sampling in steps of 2.5° reduces the accuracy of the results particularly at lower flip angles; as can be seen in Figs. 2a and 2b, the actual minimum is to be expected between the measured angles and closer to the theoretical value. (b) The (theoretical and experimental) curves at higher flip angles are very flat; thus, it is difficult to precisely determine the minimum.

Some systematic deviations of the statistical error *in vivo* at higher flip angles between 25° and 30° may be related to increasing involuntary subject motion towards the end of the series of measurements (even small sub-voxel head motion will increase the standard deviation of the set of pixels in the difference image data). Considering all our results from MRI measurements, the chosen approach for flip-angle optimization was fully justified by experimental data. Other, considerably more complex signal and error analysis approaches as developed by Deoni et al. (6) or Dathe and Helms (13) are not required to model the precision of the proposed 1FA approach.

The 1FA technique provides reasonably accurate T_1 values (with a maximum deviation of 10.3% for the longest T_1 and with deviations of about $\pm 3\%$ for the other measurements) compared to the standard-of-reference SR technique. For the longest T_1 , the parameter choice of the SR measurement (in particular, the longest recovery time of about 5 seconds) might not be optimal. The remaining T_1 deviations could be related to neglected T_2^* influences and imperfect B_1 correction. T_2^* effects are unavoidable at higher contrast-agent concentrations and depend on the transversal relaxivity and, in particular, also on the spatial distribution of

the contrast agent in the voxel volume. They can be reduced by minimizing the echo time (and, if possible, by avoiding too high concentrations of contrast agent).

Visually, the 1FA T_1 maps agree well with the SR T_1 maps (cf. Fig. 3). The SR acquisition of the liquid with longest T_1 visually suffered from some motion-induced flow (convection), which is probably the reason for the remaining systematic differences of T_1 when comparing the SR and the 1FA results.

The present study was performed with a series of relatively slow conventional 3D FLASH acquisitions (temporal resolution of about 40 s/volume). However, it can easily be implemented with ultra-fast dynamic acquisition techniques such as TRICKS (14) or TWIST (15), which dramatically improve the temporal resolution of T_1 mapping to the order of about 1 s/volume. Further improvements of the proposed techniques might include the dynamic adjustment of the optimal flip angle during the measurement based on real-time-evaluated T_1 estimates in a region or volume of interest.

Generally, the proposed technique suffers from the same limitations as all VFA-related approaches for T_1 mapping. Systematic errors are caused, e. g., by B_1 inhomogeneities, particularly at higher field strengths of 3 Tesla or more. These effects can be reduced either by more homogeneous B_1 excitation using, e. g., parallel-transmit techniques (16, 17), or by correction techniques based on B_1 measurements as in the present study (10). Another difficulty of VFA-based T_1 mapping are spoiling-related errors as analyzed in detail by Yarnykh (18). Both effects may have influenced the accuracy of the presented T_1 values and need to be considered for accurate T_1 mapping; however, our main result, i. e., the dependence of the statistical error on the flip angle, is not directly influenced by these effects. System (or signal) stability can be a limiting factor for the accuracy of T_1 measurements particularly in very long dynamic acquisitions: all dynamic acquisitions are evaluated based on the initial baseline measurements; consequently, any long-term signal drift will be reflected by biased T_1 values. Thus, for very long measurements (over, e. g., more than 5 minutes) the proposed technique may be used only, if the system is known to provide excellent temporal signal stability; otherwise, conven-

tional VFA T_1 measurements (based on at least 2 different flip angles for each dynamic phase) may be preferable – at least for later phases, in which the dynamic change of T_1 is typically much slower than in the first part (arterial phase) of the measurement.

Conclusions

Fast dynamic T_1 mapping with optimal precision is feasible acquiring only a single 3D FLASH data set for each time point in combination with a longer baseline measurement. The optimal flip angle for the dynamic series can be determined by averaging $\alpha_{\text{dyn,opt}} = \arccos[(2E_1 - 1)/(2 - E_1)]$ over the expected range of T_1 values.

References

1. Crawley AP, Henkelman RM. A comparison of one-shot and recovery methods in T1 imaging. *Magn Reson Med* 1988;7:23-34.
2. Look DC, Locker DR. Time saving in measurement of NMR and EPR relaxation times. *Rev Sci Instrum* 1970;41:250-251.
3. Kay I, Henkelman RM. Practical implementation and optimization of one-shot T1 imaging. *Magn Reson Med* 1991;22:414-424.
4. Haase A. Snapshot FLASH MRI. Applications to T1, T2, and chemical-shift imaging. *Magn Reson Med* 1990;13:77-89.
5. Fram EK, Herfkens RJ, Johnson GA, Glover GH, Karis JP, Shimakawa A, Perkins TG, Pelc NJ. Rapid calculation of T1 using variable flip angle gradient refocused imaging. *Magn Reson Imaging* 1987;5:201-208.
6. Deoni SC, Rutt BK, Peters TM. Rapid combined T1 and T2 mapping using gradient recalled acquisition in the steady state. *Magn Reson Med* 2003;49:515-526.
7. Ingrisch M, Sourbron S. Tracer-kinetic modeling of dynamic contrast-enhanced MRI and CT: a primer. *J Pharmacokinetic Pharmacodyn* 2013;40:281-300.
8. Brookes JA, Redpath TW, Gilbert FJ, Needham G, Murray AD. Measurement of spin-lattice relaxation times with FLASH for dynamic MRI of the breast. *Br J Radiol* 1996;69:206-214.
9. Ernst RR, Anderson WA. Application of Fourier transform spectroscopy to magnetic resonance. *Rev Sci Instrum* 1966;37:93-102.
10. Yarnykh VL. Actual flip-angle imaging in the pulsed steady state: a method for rapid three-dimensional mapping of the transmitted radiofrequency field. *Magn Reson Med* 2007;57:192-200.
11. Smith SM. Fast robust automated brain extraction. *Hum Brain Mapp* 2002;17:143-155.
12. Bland JM, Altman DG. Statistical methods for assessing agreement between two methods of clinical measurement. *Lancet* 1986;1:307-310.
13. Dathe H, Helms G. Exact algebraization of the signal equation of spoiled gradient echo MRI. *Phys Med Biol* 2010;55:4231-4245.
14. Korosec FR, Frayne R, Grist TM, Mistretta CA. Time-resolved contrast-enhanced 3D MR angiography. *Magn Reson Med* 1996;36:345-351.

15. Song T, Laine AF, Chen Q, Rusinek H, Bokacheva L, Lim RP, Laub G, Kroeker R, Lee VS. Optimal k-space sampling for dynamic contrast-enhanced MRI with an application to MR renography. *Magn Reson Med* 2009;61:1242-1248.

16. Schmitter S, Wu X, Adriany G, Auerbach EJ, Ugurbil K, Van de Moortele PF. Cerebral TOF angiography at 7T: Impact of B1+ shimming with a 16-channel transceiver array. *Magn Reson Med* 2013. DOI: 10.1002/mrm.24749 (epub ahead of print)

17. Childs AS, Malik SJ, O'Regan DP, Hajnal JV. Impact of number of channels on RF shimming at 3T. *MAGMA Magn Reson Mater Phy* 2013;26:401-410.

18. Yarnykh VL. Optimal radiofrequency and gradient spoiling for improved accuracy of T1 and B1 measurements using fast steady-state techniques. *Magn Reson Med* 2010;63:1610-1626.